

Magnetic Field Seeding by Galactic Winds

Serena Bertone^{1,2*}, Corina Vogt^{3,2†} & Torsten Enßlin^{2‡}

¹*Astronomy Centre, University of Sussex, Brighton, BN1 9QH, United Kingdom*

²*Max Planck Institut für Astrophysik, Karl Schwarzschild Str. 1, 85741 Garching bei München, Germany*

³*Stichting ASTRON, P.O. Box 2, NL-7990 AA Dwingeloo, The Netherlands*

Submitted to MNRAS

ABSTRACT

The origin of intergalactic magnetic fields is still a mystery and several scenarios have been proposed so far: among them, primordial phase transitions, structure formation shocks and galactic outflows. In this work we investigate how efficiently galactic winds can provide an intense and widespread “seed” magnetisation. This may be used to explain the magnetic fields observed today in clusters of galaxies and in the intergalactic medium (IGM). We use semi-analytic simulations of magnetised galactic winds coupled to high resolution N-body simulations of structure formation to estimate lower and upper limits for the fraction of the IGM which can be magnetised up to a specified level. We find that galactic winds are able to seed a substantial fraction of the cosmic volume with magnetic fields. Most regions affected by winds have magnetic fields in the range $10^{-12} < B < 10^{-8}$ G, while higher seed fields can be obtained only rarely and in close proximity to wind-blown galaxies. These seed fields are sufficiently intense for a moderately efficient turbulent dynamo to amplify them to the observed values. The volume filling factor of the magnetised regions strongly depends on the efficiency of winds to load mass from the ambient medium. However, winds never completely fill the whole Universe and pristine gas can be found in cosmic voids and regions unaffected by feedback even at $z = 0$. This means that, in principle, there might be the possibility to probe the existence of primordial magnetic fields in such regions.

Key words: cosmology: theory – intergalactic medium – magnetic fields – galaxies

1 INTRODUCTION

The investigation of magnetic fields in the intergalactic medium (IGM) and in the intracluster medium (ICM) is a new challenge for modern cosmology. While magnetic fields have been successfully detected in clusters of galaxies using a variety of techniques, such as Faraday rotation measurements and observations of diffuse large-scale synchrotron emission (for recent reviews see Carilli & Taylor 2002; Widrow 2002; Govoni & Feretti 2004), only a handful of pioneering observations suggest that magnetic fields of significant intensity may be present in the IGM¹ and no accurate measurements are available for those regions of the

Universe with densities of order of the mean cosmic density or lower.

Cluster magnetic fields detected through Faraday rotation measurements are of the order of a few μ G. Kim et al. (1990) measured field strengths of about 2 μ G on scales of 10 kpc in a statistical sample of point sources observed through the Coma cluster, and Clarke, Kronberg and Böhringer (2001) derived field strengths of 4 to 8 μ G in a sample of point sources observed in 16 low redshift clusters. Johnston-Hollitt & Ekers (2004) have done a similar analysis of southern galaxy clusters and provided an independent confirmation of the statistical signal reported by Clarke et al. (2001). Magnetic field strengths of 10 to 40 μ G have been reported for the cool cores of the Hydra A and Cygnus A clusters on scales of 3–5 kpc (Dreher, Carilli & Perley 1987, Taylor & Perley 1993). Vogt & Enßlin (2005) apply a maximum likelihood estimator for magnetic power spectra, based on the theory of turbulent Faraday screens (Enßlin & Vogt 2003; Vogt & Enßlin 2003), to a high quality Faraday rotation map of the north lobe of the radio source Hydra A produced by the

* E-mail: s.bertone@sussex.ac.uk

† E-mail: vogt@astron.nl

‡ E-mail: ensslin@mpa-garching.mpg.de

¹ We define the intracluster medium (ICM) as the gas bound to clusters and groups of galaxies, while we call intergalactic medium (IGM) the diffuse gas in the Universe which is not bound to any such structure. This distinction is clear in numerical simulations, but it may not always be so in observations.

novel PACERMAN algorithm (Dolag, Vogt & Enßlin 2005; Vogt, Dolag & Enßlin 2005). They find a cluster central magnetic field strength of $7 \pm 2 \mu\text{G}$.

There have been few attempts to detect intergalactic magnetic fields beyond clusters. Kim et al. (1989) detected radio-synchrotron radiation from an extended magnetic field in the region of the Coma supercluster, with a field strength of 0.1 to $0.01 \mu\text{G}$. This radio emission comes from a region with an enhanced number density of galaxies, which might indicate a group of galaxies in the process of merging with Coma. Bagchi et al. (2002) report possible radio-synchrotron evidence of intergalactic magnetic fields in the region ZwCL 2341.1+0000 at $z \sim 0.3$, where galaxies seem to be aligned along a filament. However, in both cases it remains controversial whether these measurements prove the magnetisation of the diffuse IGM or instead the state of the gas belonging to the supercluster environment.

Theoretically, three basic mechanisms could explain the presence of magnetic fields in the ICM and IGM (for a review Widrow 2002): i) they could have a primordial origin, ii) they were seeded in the IGM by battery effects of shock waves or inhomogeneous radiation fields, or iii) their existence is linked to the formation and evolution of galaxies. A primordial origin implies that weak seed fields of about $\sim 10^{-18} \text{ G}$ were produced during the early phases of the cosmic evolution (see Rees 1987; Kronberg 1994). These seed fields must have later been amplified by extremely efficient mechanisms, if the fields we are to observe today were of the order of a fraction of a μG . Alternatively, seed magnetic fields may have been produced in protogalaxies and galaxies and subsequently ejected into the ICM and IGM. In both cases, cosmic shear and/or dynamo effects may intervene to amplify the seed fields.

Cosmological magnetohydrodynamic simulations of magnetic fields in galaxy clusters have been performed by Dolag, Bartelmann & Lesch (1999), assuming a homogeneous seed field of 10^{-9} G at $z \sim 15$. They find that seed fields of this intensity can be efficiently amplified to reproduce the magnetic field strength observed in local clusters. However, inhomogeneous seed fields can similarly lead to the right amount of cluster magnetisation: Miniati et al. (2001a) follow the evolution of the magnetic fields produced by Biermann–battery effects in shock waves from the cosmic structure formation process and find that they can be further amplified by cosmic shear flows, leading to strong cluster fields.

Two different mechanisms can explain the transport of the magnetic seed fields produced in galaxies into the ICM and the diffuse IGM. The magnetic energy may be easily ejected into the IGM and ICM by jets and radio lobes emerging from powerful radio galaxies (Hoyle 1969; Rees 1987; Daly & Loeb 1990; Chakrabarti, Rosner & Vainshtein 1994). Enßlin et al. (1997) estimated the injection of magnetic fields by radio galaxies, and Völk & Atoyan (2000) followed the subsequent amplification through dynamo effects, finding that it can account quite accurately for the observed magnetic field strengths and cosmic ray densities in the ICM. Kronberg et al. (2001) make a step further and estimate the magnetic flux transported directly into the IGM. The second mechanism is related to the ejection of magnetised interstellar gas and supernova ejecta by galactic winds. Kronberg, Lesch & Hopp (1999) consider such a scenario of

magnetised outflows from star forming galaxies and find that a substantial fraction of the intergalactic medium could have been seeded at relatively high redshift. However, their estimate was based on a power-law extrapolation of the cosmic star formation rate to high redshifts, which is not consistent with the known peak of star formation activity at $z \sim 1$ (Madau et al. 1996). De Young (1992) follows the amplification of a variety of magnetic seed fields by turbulent dynamo, driven by the motion of galaxies in the ICM, and concludes that this mechanism cannot account for the magnetic fields observed in clusters.

Galactic winds emerging from star forming galaxies have been detected throughout the history of the Universe (e.g. Phillips 1993, Heckman et al. 2000, Cecil, Bland-Hawthorn & Veilleux 2002, Frye, Broadhurst & Benitez 2002, Adelberger et al. 2003, Veilleux, Cecil & Bland-Hawthorn 2005) and are often advocated to explain the metal enrichment of the IGM (e.g. Aguirre et al. 2001; Theuns et al. 2002; Bertone, Stoehr & White 2005, BSW05 hereafter). Although it is still controversial if winds from large galaxies can fully account for the observed level of metal enrichment of the IGM at $z \sim 3$ (Aguirre et al. 2005), it is clear that they do play a role in galaxy formation and there is no doubt whether they eject a consistent fraction of the metal and gas content of galaxies at any redshift.

Magnetic fields are clearly observed in the interstellar medium of galaxies (Beck 2001), where they are believed to play an essential role during star formation. In a few cases, magnetic fields are also observed in the galactic material outflowing from star forming galaxies (Reuter et al. 1994; Golla & Hummel 1994; Tüllmann et al. 2000). Reuter et al. (1992) estimate a magnetic field strength of $10 \mu\text{G}$ in the material outflowing from M82, while Dahlem et al. (1997) find a field strength of about $7 \mu\text{G}$ in the outflow of NGC 4666. Birk, Wiechen & Otto (1999) argue that galactic winds are able not only to advect galactic magnetic fields but also to amplify them by shear flows from Kelvin–Helmholtz instability. If a significant fraction of the outflows are magnetised, it is reasonable to expect that they may at least partially contribute to the magnetisation of the ICM and IGM. The transport of the magnetic flux by galactic outflows may occur at virtually any redshift: at higher redshifts the main contribution may come from protogalaxies with total masses of the order of $\gtrsim 10^6 \text{ M}_\odot$, while at lower redshifts galaxies with stellar masses comparable to the ones of local dwarf galaxies or larger may become the dominant source of magnetic fields.

In this paper, we use high resolution simulations of galaxy formation, which include semi-analytic prescriptions for the physics of galactic winds, to investigate the efficiency of outflows to seed the ICM and IGM with magnetic fields and cosmic rays. Numerical models of galactic winds do partially explain the transport of the metals produced in galaxies into the IGM and, since there is an analogy between the transport of metals and the transport of magnetic fields, we investigate the possibility that galactic winds can eject seed magnetic fields from galaxies and transport them into the IGM and ICM. However, we do not intend to investigate in detail all the physical phenomena connected to the transport of the magnetic fields in our simulations, because

semi-analytic models are intrinsically not suitable to treat the magneto-hydrodynamics involved in full detail.

We present two different scenarios for the ejection and transport of magnetic fields by galactic winds: a “conservative” scenario and an “optimistic” scenario. For each case, we then analyse the effect of the efficiency of winds to affect the results. In the first scenario, we aim to provide a “conservative” estimate of the global magnetisation of the Universe and we only consider the ejection and the transport of magnetic “seed” fields by winds, while amplification mechanisms are neglected. As a consequence, these results should be treated as lower limits. In the second scenario, we include a simple prescription for the amplification of the seed magnetic fields during the wind evolution and we predict a level for the magnetisation of the Universe that represents an extreme case and that can be therefore regarded as an upper limit.

Given the resolution of our simulations, we focus on the evolution of winds emerging from galaxies with $M_\star \gtrsim 10^8 M_\odot$ at $z \lesssim 10$. We are interested in determining the fraction in volume of the ICM and IGM which can be magnetised by winds and we calculate the minimum magnetic energy and the minimum cosmic ray energy density which can be ejected into the ICM and IGM by winds.

The paper is organised as follows. In Section 2 we describe our set of simulations and how we implement our recipes for the transport and amplification of the seed magnetic fields on top of the prescriptions for the evolution of galactic winds. In Section 3 we present our results for the transport of magnetic fields by winds and we discuss the possible amplification of the seed fields by cosmic shear and turbulence. We briefly discuss the ejection, transport and amplification of cosmic rays in Section 4 and finally we draw our conclusions in Section 5.

2 THE SIMULATIONS

In this work, we use the simulations of galactic winds presented in BSW05 and we implement new semi-analytic recipes for the transport of the magnetic fields on top of the pre-existing scheme. We assume a Λ CDM cosmology with matter density $\Omega_m = 0.3$, dark energy density $\Omega_\Lambda = 0.7$, Hubble constant $h = 0.7$, primordial spectral index $n = 1$ and normalisation $\sigma_8 = 0.9$.

In Subsection 2.1 we briefly describe the set of high resolution N-body simulations and the semi-analytic model for galaxy formation. We present our prescriptions for the physics of galactic winds in Subsection 2.2 and for the evolution of magnetic fields and cosmic rays in Subsections 2.3 and 4.1, respectively.

2.1 Formation and Evolution of Galaxies

A set of high resolution N-body simulations, “M3” (Stoehr 2003), is used to follow the evolution of the dark matter and the formation of structures with time. The “field” simulation M3 describes an approximately spherical region of space with diameter $52 h^{-1}$ Mpc and average density close to the cosmic mean. The fact that only about half the enclosed galaxies at $z = 0$ are field galaxies, while the rest are in groups and poor clusters, makes it particularly suitable

to investigate the effects of feedback on the diffuse IGM. The M3 simulation efficiently combines a high resolution in mass with a large simulated volume, necessary to study the effects of feedback from galaxies with stellar masses as low as dwarfs in their proper cosmological context. The number of particles in the simulated region is about $7 \cdot 10^7$ and the particle mass is $1.7 \cdot 10^8 h^{-1} M_\odot$. The simulations were performed by Stoehr (2003) using the parallel treecode GADGET I (Springel, Yoshida & White 2001). The dark matter evolution was followed from redshift $z = 120$ down to redshift $z = 0$ and 52 simulation outputs were stored between $z = 20$ and $z = 0$.

The formation and evolution of galaxies is modelled with the semi-analytic technique proposed by Kauffmann et al. (1999) in the new implementation by Springel et al. (2001). Merging trees extracted from the simulations are used to follow the galaxy population in time, while simple prescriptions for gas cooling, star formation and galaxy merging model the processes involving the baryonic component of the galaxies. At $z = 3$ a total of about four hundred thousand galaxies are identified and about three hundred and fifty thousand are present at $z = 0$. The two largest clusters have a total mass of about $10^{14} h^{-1} M_\odot$.

2.2 Prescriptions for Galactic Winds

BSW05 implement new prescriptions for the long-term evolution of winds in the semi-analytic code of Springel et al. (2001). Their model aims to provide simple predictions about the effects of winds on the diffuse IGM and, in particular, on its metal enrichment history. Here, we give a brief qualitative description of the model, but we refer the interested reader to BSW05 for a more detailed discussion.

The dynamics of galactic winds is modelled as a two-phase process: a pressure-driven, adiabatic phase, followed by a momentum-driven phase. We treat these two phases separately, according to the different physical processes that drive the expansion of winds. During the first phase, an over-pressurised bubble of hot gas emerges from a star forming galaxy and evolves adiabatically until its cooling time becomes shorter than its dynamical expansion time. This Sedov-Taylor phase of the evolution terminates when the loss of energy by radiation becomes substantial and the material at the outer edge of the bubble starts to cool down. During the second phase of the wind evolution, a thin shell of cooled material accumulates at the shock front and the dynamics of the wind becomes dominated by the momentum imparted by the outflowing material onto the thin shell. This second phase is the classic momentum-driven snowplough and both the shell and the outflowing wind material are cool. For simplicity, we make the assumption of spherical symmetry.

According to Ostriker & McKee (1988), during the Sedov-Taylor phase of adiabatic expansion the dynamics of the outflow is described by the equation for the conservation of energy of a spherical bubble with energy injection at the origin:

$$\frac{dE_w}{dt} = \frac{1}{2} \dot{M}_w v_w^2 + \varepsilon 4\pi R^2 \cdot \left\{ \left[\frac{1}{2} \rho_o v_o^2 + u_o - \rho_o \frac{GM_H}{R} \right] (v_s - v_o) - v_o P_o \right\} \quad (1)$$

where E_w is the wind energy, R and v_s are the radius and the velocity of the shock, \dot{M}_w and v_w the mass outflow rate and the outflow velocity of the wind, ρ_o , P_o , v_o and u_o the density, the pressure, the outward velocity and the internal energy of the surrounding medium, respectively. M_H is the total mass internal to the shock radius. The entrainment fraction ε is a parameter that defines the fraction of mass that the bubble sweeps up while crossing the ambient medium. This equation states that the bubbles are powered by the material outflowing from the galaxies and that they are slowed down by gravity and by the ram pressure and the thermal pressure of the ambient medium.

The equation of motion for a spherically symmetric thin shell is given by the conservation of momentum (Ostriker & McKee 1988):

$$\frac{d}{dt}(mv_s) = \dot{M}_w(v_w - v_s) - \frac{d\phi}{dR}m - \varepsilon 4\pi R^2 P_o - \varepsilon 4\pi R^2 \rho_o v_o (v_s - v_o), \quad (2)$$

with m , R and v_s the mass, the radius and the velocity of the shell and ϕ the gravitational potential of the dark matter halo. The first term on the right-hand side represents the momentum injected by the starburst, the second term takes into account the gravitational attraction of the dark matter halo and the two final terms represent the thermal and the ram pressure of the surrounding medium.

The conservation of mass law for a pressure driven bubble is

$$\frac{dM}{dt} = \dot{M}_w + \varepsilon 4\pi R^2 \rho_o (v_s - v_o), \quad (3)$$

while for a thin shell

$$\frac{dm}{dt} = \dot{M}_w \left(1 - \frac{v_s}{v_w}\right) + \varepsilon 4\pi R^2 \rho_o (v_s - v_o). \quad (4)$$

Initial conditions for the mass loss rate and the velocity of winds are taken from Shu, Mo & Mao (2005) and calibrated to match the observations of winds both in local starbursts and in high redshift galaxies (e.g. Martin 1999, Frye, Broadhurst & Benitez 2002). \dot{M}_w and v_w are calculated as a function of the star formation rate of the galaxy blowing the wind:

$$\dot{M}_w = 5 \cdot \dot{M}_\star^{0.71} K \text{ M}_\odot \text{ yr}^{-1}, \quad (5)$$

$$v_w = 320 \cdot \dot{M}_\star^{0.145} K^{-1/2} \text{ km s}^{-1}, \quad (6)$$

where K is a constant that takes into account various properties of the interstellar medium (ISM) like, e.g., the efficiency of conduction relative to the thermal conductivity of clouds, the minimum radius of clouds in the ISM and the dimension of star-forming regions (see Shu, Mo & Mao 2005 for a comprehensive discussion). With this assumption, the momentum input $\dot{M}_w v_w$ is only weakly dependent on K ($\propto K^{1/2}$), with a stronger dependence on the star formation rate ($\propto \dot{M}_\star^{0.855}$). The energy input is proportional to the star formation rate, but does not depend on K and therefore on all other galaxy properties.

Both K and ε define the mass loading of winds, but while K determines the amount of gas entrained from the ISM of the galaxy, ε is the fraction of gas swept up by winds from the ambient medium after blow out. The remaining

fraction of mass $1 - \varepsilon$ is assumed to be in dense clouds which are unperturbed by the wind. A low value $\varepsilon < 1$ may reflect either a clumpy ambient medium or a heavily fragmented wind, while $\varepsilon \sim 1$ describes a near-homogeneous medium, which can be entirely swept up by the wind. For this work we assume $K = 0.5$ and we consider two values of the entrainment fraction parameter, that is $\varepsilon = 0.1$ and $\varepsilon = 0.3$. The first value represents the behaviour of winds with inefficient mass loading, which can easily escape from galaxies at any redshift, while the second represents highly mass loaded winds, whose efficiency to expand far into the IGM is significantly reduced with respect to less mass loaded winds. BSW05 find that the results for winds only weakly depend on K , while the strongest dependence in the model is on the entrainment fraction parameter ε . Currently, there are no observational constraints on the parameter ε and our simulations are unable to constrain it on the basis of our results. Bertone & White (2005) try to constrain the parameter by comparing the statistical properties of synthetic Ly α spectra with observed ones, but are unable to put any constraint on either of the two models: both scenarios are equally likely and none is in contrast with observations. The volume filling factor of galactic winds is similarly not accurately constrained by observations: published estimates vary between 0.004% and 40% and in principle neither of the models we present in this work can be excluded on the basis of observations.

When winds expand inside the haloes of galaxy groups, they sweep up the hot and possibly metal enriched intra-group medium and they are subject to the cluster gravitational attraction, thermal and ram pressure forces. Winds expanding into the IGM entrain metal-free gas, which is assumed to have constant density and pressure and whose velocity field is determined by the Hubble flow. In principle, winds have to be far more energetic to escape from large dark matter haloes than to escape from field galaxies or small groups, since the forces they have to overcome are stronger. In general, winds have a higher probability to escape the haloes of isolated galaxies than to escape from groups, and it is unlikely that they can escape from large clusters, although we cannot prove this in our simulations because of the lack of massive dark matter haloes. Ram pressure plays an important role to quench outflows and its influence is particularly strong in large haloes, where it can prevent winds from blowing (Kapferer et al. 2006). Thermal pressure in low-redshift haloes can also slow down winds considerably, but is normally negligible with respect to the other forces at high redshifts.

2.3 Prescriptions for Magnetic Fields

The aim of our calculations is to describe the injection of seed magnetic fields into the IGM by galactic winds. With our current means, this can only be done in an approximative way. One of the main simplifications we use in the following is the assumption that the magnetic fields in winds are dynamically negligible. This does not imply that organised magnetic fields at the base of the wind could not play a role in launching the outflows. However, we assume that the conversion of magnetic forces into kinetic energy happens before the fields enter the expanding wind bubble. The remaining magnetisation evolves passively within the out-

flow, allowing a simplified description of its evolution, as we briefly describe below. A more detailed derivation of our equations is given in Appendix A.

We define the injection of the magnetic fields ejected by galaxies into the IGM as the *magnetic field seeding*, since this expression literally describes the process well. Potentially, shear flows in the IGM can subsequently amplify these seed fields to the observed levels. We note that the term *magnetic field seeding* is often used in the literature to describe the Battery–effects, which generate magnetic fields without requiring a pre-existing seed magnetization, due to corrections to the ideal magneto–hydrodynamic equations. This initial generation of magnetic fields is believed to take place in stars, in galaxies and during the early phases of the evolution of the universe. In this work, we do not attempt to model the process, but we assume that it has happened in the past, allowing galaxies to create their own magnetic field and to amplify it to the observed level. This existing magnetic field is then ejected by the galaxy and advected in to the IGM by a galactic–scale outflow.

In our conservative scenario, we treat the seed magnetic fields analogously to the metals and we do not process them any further: this implies that we describe the injection of the seed fields by galaxies into the outflows and their dilution due to the expansion of winds, but that we do not take into account any possible mechanism that could produce amplification. With this assumption, we can make predictions for the injection and transport of seed magnetic fields into the IGM and ICM, which effectively result in a lower limit of the actual magnetisation of the Universe.

We present our prescriptions for the amplification of the seed fields in Subsection 2.3.2, where we describe the build–up of our optimistic scenario. We discuss other possible mechanisms that could further amplify the seed fields transported by winds in Subsection 3.3 and we make a few consideration about the transport of cosmic rays in winds in Section 4.

2.3.1 Conservative Scenario

Since in this work we want to make order of magnitude predictions, we neglect the possible influence of the magnetic fields on the evolution of the galactic winds and we set up the new semi–analytic prescriptions for the magnetic fields on top of the pre-existing scheme of BSW05. However, this approximation turns out to be well justified: in fact, in our calculations we find that the magnetic energy is always several orders of magnitude smaller than the total energy in the winds.

To simulate the transport of magnetic fields by galactic winds, we need two main ingredients: an equation for the evolution of the magnetic fields and suitable initial conditions. To be consistent with the evolution of winds set by equations (1) and (3), we derived an equation for the evolution of the magnetic energy in winds:

$$\frac{d}{dt} E_B = \dot{E}_{B_{\text{in}}} - \frac{1}{3} \frac{\dot{V}_w}{V_w} E_B. \quad (7)$$

E_B is the total magnetic energy in a bubble, $\dot{E}_{B_{\text{in}}}$ is the rate of magnetic energy injected by winds, V_w is the wind volume and \dot{V}_w is the variation in the wind volume due to the expansion. The second term on the right hand side of equation

(7) expresses the decrease in the magnetic energy due to the adiabatic expansion of the bubbles and is a negative contribution. This can be deduced from the induction equation for a frozen–in magnetic field expanding isotropically, when the shear amplification term is neglected. A detailed derivation, which discusses the underlying assumptions, can be found in Appendix A. Here we give a simplified argument. The induction equation yields $B \propto 1/R^2$ and $E_B \propto V B^2 \propto 1/R$. This implies that

$$\frac{d}{dt} E_B \propto -E_B \frac{v_s}{R} \propto \frac{1}{3} \frac{\dot{V}_w}{V_w}, \quad (8)$$

where the numerical factor 1/3 reflects the assumption of no special alignment between the local field direction and the local direction of the expansion of the wind.

We assume that the magnetic energy injection rate is

$$\dot{E}_{B_{\text{in}}} = \varepsilon_{B_{\text{in}}} \frac{\dot{M}_w}{\bar{\rho}_{\text{in}}} = \varepsilon_{B_{\text{in}}} \dot{V}_{\text{in}}, \quad (9)$$

where \dot{V}_{in} is the volume of the injected material, $\bar{\rho}_{\text{in}}$ is the density of the gas injected into the wind, $\varepsilon_{B_{\text{in}}}$ is the magnetic energy density of the wind material outflowing from the galaxy, and the mass outflow rate \dot{M}_w is given by equation (5). Equation 9 assumes that the magnetic field injected at the base of the wind has the strength of a typical galactic magnetic field. Since the production of a galactic–scale magnetic field by, for example, an $\alpha - \Omega$ dynamo mechanism is not instantaneous, we assume that in our simulations magnetic energy can be injected in winds only after the host galaxy has completed a full rotation. The rotational period of the galaxy is calculated as a function of the disk radius and circular velocity, that is $t_{\text{rot}} = 2\pi R_g/v_c$.

In our model, winds make a transition between the pressure driven phase and the momentum driven phase when their cooling time becomes shorter than their dynamical timescale. However, when simulating the evolution of the magnetic fields in the wind, we continue to use equation (7) for the conservation of the magnetic flux throughout the wind evolution. This is a reasonable approximation, because the magnetic energy can be injected into the winds independently of the dynamical phase of the wind and equation (7) does not critically depend on any quantity linked to a particular phase of the wind.

A crucial quantity in Eq. (9) is the density $\bar{\rho}_{\text{in}}$ of the gas outflowing from a galaxy at a rate \dot{M}_w . A estimate of this quantity can be derived as a function of the mass loss rate \dot{M}_w of a wind through the entire surface area $4\pi R_g^2$ of a galaxy at the velocity v_w :

$$\bar{\rho}_{\text{in}} = \frac{\dot{M}_w}{4\pi R_g^2 v_w}, \quad (10)$$

where we assume that the galactic radius is a fixed fraction of the virial radius, that is $R_g = R_{200}/10$, as in BSW05. The magnetic energy density $\varepsilon_{B_{\text{in}}}$ associated with the mass injected in winds can be expressed as

$$\varepsilon_{B_{\text{in}}} = \frac{B_{\text{gal}}^2}{8\pi} \left(\frac{\bar{\rho}_{\text{in}}}{\bar{\rho}_{\text{ISM}}} \right)^{4/3}, \quad (11)$$

with B_{gal} the galactic magnetic field and $\bar{\rho}_{\text{ISM}}$ the density of the interstellar medium (ISM) of the galaxy. Here we assume that the magnetic field lines expand adiabatically and isotropically when the ISM is blown out of the disk of a

galaxy and is injected into a wind. The factor in parentheses in Eq. (11) represents therefore the dilution of the magnetic fields when the density of the ejected gas drops below the density of the ISM. The adiabatic index 4/3 derives from the relationship $B \propto 1/R^2$ in the induction equation, which implies $B \propto \rho^{2/3}$ and $B^2 \propto \rho^{4/3}$ for isotropic expansion. The density of the ISM is given by

$$\bar{\rho}_{\text{ISM}} = \frac{3M_{\text{ISM}}}{4\pi R_g^3}, \quad (12)$$

with M_{ISM} the mass of the ISM.

Galaxies in the local Universe have magnetic fields of order 5 μG (e.g. Dahlem et al. 1997, Chyží et al. 2003), while interacting galaxies can have magnetic fields as high as 30 μG (e.g. Soida et al. 2001, Chyží & Beck 2004, Harnett et al. 2004). In our simulations, we will express

$$B_{\text{gal}} = b \cdot B, \quad (13)$$

where $B = 1 \mu\text{G}$ is a conservative reference magnetic field value at the base of the winds and b is a “fudge” factor to rescale our results to less conservative choices of an initial magnetic field.

2.3.2 Optimistic scenario

In this Subsection we describe our simple and purposefully optimistic prescription for the amplification of magnetic fields during the wind evolution. To set up this prescription, we consider only the amplification caused by two mechanisms directly linked to the wind evolution, namely the injection of the shocked interstellar gas into the wind and the expansion of the wind into the surroundings of the source galaxy.

The first mechanism we consider is the amplification of the magnetic fields at the base of the winds, where the outflowing material escapes the visible regions of galaxies. Here, the magnetic fields embedded in the ejected gas can be amplified through Kelvin–Helmholtz instabilities. This complex process is described in detail by Birk, Wiechen & Otto (1999) and we do not intend to discuss it further. What is relevant for this work is the fact that Birk, Wiechen & Otto (1999), when simulating the process, find that the magnetic energy density increases by a factor of 3, almost independently of their set of initial conditions. We take this into account in our simulations by scaling the magnetic field we inject in winds by the fudge factor $b = \sqrt{3}$ in Eq. (13). In addition, we do know that observations of magnetic fields in local galaxies yield strengths of about $B_{\text{gal}} \sim 6 \mu\text{G}$ (e.g. Beck 2001; Dahlem et al. 1997; Chyží et al. 2003). For our optimistic scenario, we therefore set the magnetic field strength associated to the galactic ISM to be $B_{\text{gal}} = 6 \mu\text{G}$. If we incorporate this value of a more realistic galactic magnetic field in the fudge factor, together with the amplification factor of $\sqrt{3}$ at the base of the wind by Kelvin–Helmholtz instability, we obtain a total fudge factor $b = 10$, which we include in our simulations.

The second mechanism we consider for the amplification of magnetic fields is the effect of shear flows inside wind cavities and bubbles during the wind expansion into the ambient medium. To estimate how strongly the magnetic fields could be amplified, we first need to determine the characteristic timescale of this mechanism. Since motions inside winds

can take place on scales of the order of the wind radius R , an effective timescale τ_{eff} can be estimated as

$$\tau_{\text{eff}}^{-1} = \eta \frac{v_s - v_H}{R} = \eta \left(\frac{v_s}{R} - H(t) \right), \quad (14)$$

where v_s is the proper wind expansion velocity, $v_H = H(t) \cdot R$ is the Hubble flow at distance R from the source galaxy and $H(t)$ is the Hubble constant as a function of time. The term $v_s - v_H$ represents the peculiar velocity of a wind with respect to the Hubble flow and is the only shear motion whose contribution to the amplification of the magnetic field in wind we consider. η is a field amplification efficiency factor which depends on the poorly known flow geometry inside the wind. This amplification by shear motions directly counteracts the dilution of the magnetic fields due to the adiabatic expansion term and can be incorporated in Eq. 7 for the evolution of the magnetic energy as a positive term:

$$\frac{d}{dt} E_B = \dot{E}_{B_{\text{in}}} + \left(\frac{1}{\tau_{\text{eff}}} - \frac{1}{3} \frac{\dot{V}_w}{V_w} \right) E_B. \quad (15)$$

If we assume that $\eta = 1$ and we remember that the ratio $\dot{V}_w / (3V_w)$ can be expressed as v_s/R , Eq. 15 simplifies to

$$\frac{d}{dt} E_B = \dot{E}_{B_{\text{in}}} - H(t) E_B. \quad (16)$$

In this extremely optimistic case in which $\eta = 1$, the dilution of the magnetic fields by adiabatic expansion and the amplification by shear motions cancel out, leaving behind only the term $H(t) E_B$. This factor is small with respect to the magnetic energy injection term $\dot{E}_{B_{\text{in}}}$ and it therefore represents only a small correction in Eq. 16.

3 RESULTS

In this Section we show our results for the magnetisation of the IGM and ICM. In Subsection 3.1 we discuss the simulated properties of the magnetic fields in winds for the conservative and the optimistic scenarios. In Subsection 3.2 we present our results for the fraction of magnetised IGM as a function of cosmic time and we qualitatively describe the effect of galaxy clustering on the distribution of the magnetic fields in our simulated region. We present our results in terms of *comoving* magnetic field strengths, as it is usually done in the community. Since our simulations produce physical estimates of the magnetic fields, we use the relation $B_{\text{comoving}} = B_{\text{physical}} / (1+z)^2$ to convert from one system of reference to the other.

In the following Subsections, all results are presented for a total of four different models, which we list here for convenience. The first two models represent our conservative scenario and correspond to two different wind efficiencies: the “ $\varepsilon = 0.1$ ” model represents the case of efficient winds and the “ $\varepsilon = 0.3$ ” model the case of less efficient winds. There are then two additional models which represent our optimistic scenario. In the following, they will be referred to as the “ $\varepsilon = 0.1A$ ” model and the “ $\varepsilon = 0.3A$ ” model and they correspond to efficient and less efficient wind models respectively.

3.1 Magnetic Fields and Cosmic Rays in Winds

Before describing our main results for the magnetisation of the IGM, we focus briefly on the properties of the magnetic

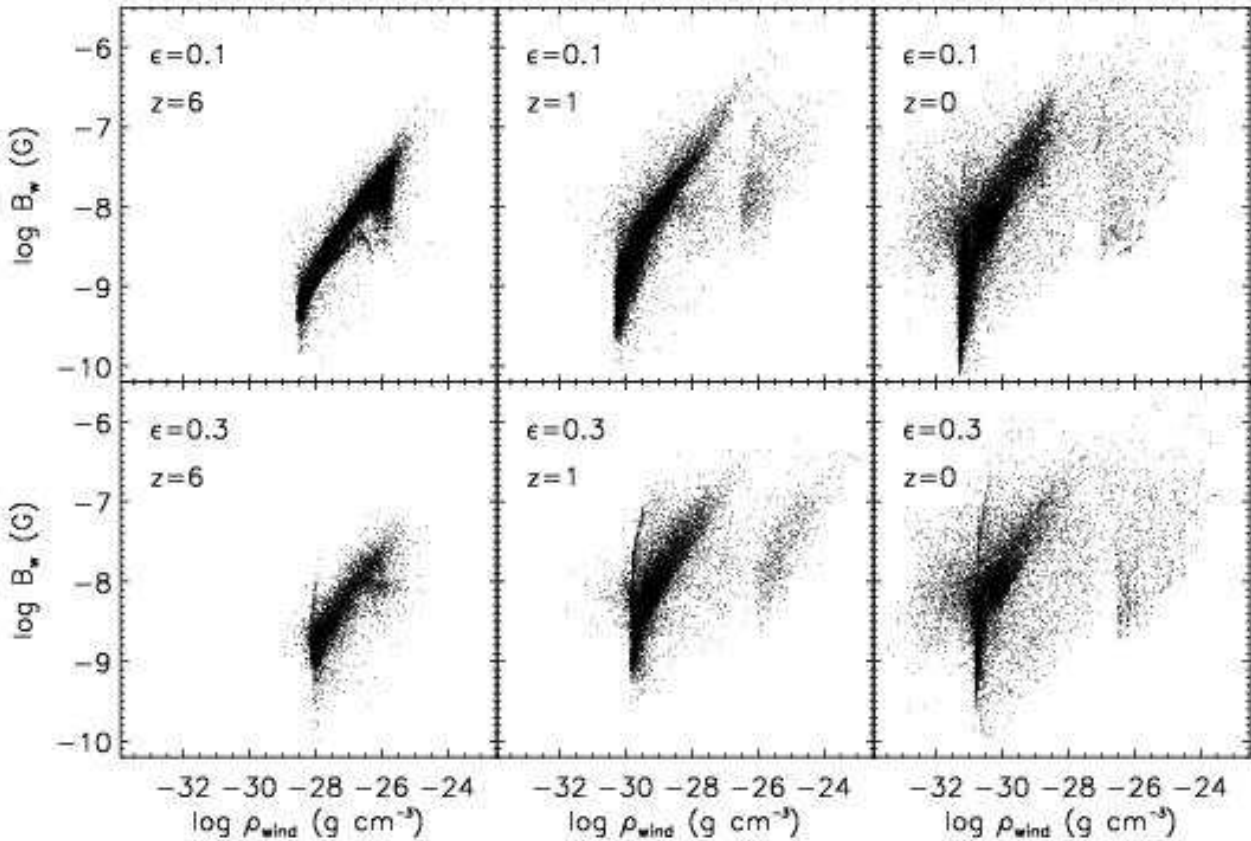


Figure 1. The magnetic field strength B_w for the conservative scenario in winds as a function of the wind density for three different redshifts ($z = 6$, $z = 1$ and $z = 0$, from left to right) and for our two wind models with $\epsilon = 0.1$ (upper panels) and $\epsilon = 0.3$ (lower panels) in the conservative scenario.

fields in winds as they emerge from our simulations. Our semi-analytic model computes the total magnetic energy in a wind E_B , which can easily be transformed in the root mean squared magnetic field strength B_w by the equation:

$$E_B = \frac{B_w^2}{8\pi} \cdot \frac{4\pi}{3} R^3, \quad (17)$$

with R the wind radius. B_w should be regarded as a root mean square magnetic field strength within the wind rather than as the value of a uniform magnetic field.

We find that B_w depends on several factors: among them, the wind density and the total magnetic energy injected by the starburst. Consistently, we never observe values of B larger than $1 \mu\text{G}$ in our conservative scenario, which means that the dilution of the field lines due to the expansion of the wind is a significant effect at any stage of the wind evolution.

In Fig. 1, we use the two wind models in our conservative scenario to show the comoving magnetic field strength in individual winds as a function of the wind density. Results are presented for three different redshifts ($z = 6$, $z = 1$ and $z = 0$, from left to right) and for our two wind models with $\epsilon = 0.1$ (upper panels) and $\epsilon = 0.3$ (lower panels). Each point represents a wind at the particular snapshot time. The total number of winds is between about 10^4 and about $3 \cdot 10^5$, depending on the redshift and on the model. There is a clear

trend that indicates that B_w increases with the wind density. The scatter is mostly due to the different stages of evolution of each wind: most winds are currently expanding into the IGM, but a number of them are recollapsing onto the galaxies, a phenomenon known as galactic fountain. Winds outflowing from galaxies which have only recently assembled most of their mass may not be magnetised, since the galaxy may not have had time to build up a magnetic field (see Subsection 2.3). In Fig. 1, the scattered points on the right-hand side of the distributions of magnetic fields indicate newly formed bubbles. These winds, which are still expanding in proximity of galaxies, normally have higher densities and their magnetic field strengths B_w depend more sensitively on the magnetisation of the material outflowing from the ISM of the galaxy. Young winds may have low B_w when little magnetic energy is injected by the starburst because the wind mass loss rate is small. However, in a few cases, when the wind mass loss rate is substantial, they may also be highly magnetised (see the points in the upper right corner of the distribution). The points corresponding to the lowest wind densities belong either to weakly magnetised winds or, in most cases, to winds which have joined the Hubble flow. By changing the fudge factor b in the expression for B_{gal} , the results in Fig. 1 can be rescaled by the same factor b .

In Fig. 2 we show the volume averaged RMS magnetic field strength in the Universe B^{RMS} (left y axis) and the

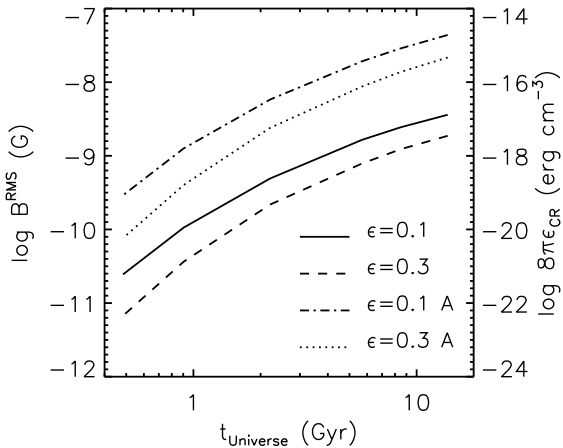


Figure 2. The volume averaged RMS comoving magnetic field (left axis) and the cosmic ray energy density (right axis, see Subsection 4.1) in winds as a function of time for the two different scenarios and the two values of our wind model parameter ϵ . If the input parameter B_{in} is modified by a fudge factor b , the results presented here for the cosmic RMS magnetic field strength can be rescaled by the same factor b , while the magnetic energy density can be rescaled by a factor b^2 .

volume averaged cosmic ray energy density ϵ_{CR} (right y axis) as a function of the cosmic time. The cosmic ray energy density has the same behaviour as magnetic field strength because we assume the magnetic and the cosmic ray energy densities to be in equipartition. Results are presented for the optimistic and the conservative scenarios and for our two wind models.

The volume averaged RMS value of the cosmic magnetic fields increases with time in both scenarios and for both wind models, in agreement with the trend we observe in Fig. 1 for the mean value of the magnetic fields in individual winds. As expected, the magnetic field strength increases more strongly in the optimistic scenario than in the conservative scenario: this is a consequence of the fact that in this scenario the dilution of the magnetic fields in winds because of the adiabatic expansion is largely compensated by the internal shear amplification.

Fig. 2 also shows that the level of magnetisation of the Universe depends critically on the efficiency of winds to transport matter, cosmic rays and magnetic energy out and far from galaxies. As stated in Subsection 2.2, the winds in models with $\epsilon = 0.1$ are much more efficient in blowing out of galaxies than in other models. As a consequence, the level of magnetisation of the Universe produced in this model is more than an order of magnitude larger than in the $\epsilon = 0.3$ models.

3.2 Volume Filling Factors of Magnetic Fields

In this Subsection we present our results for the volume filling factors of magnetised regions. By volume filling factor we mean the fraction of our simulated region affected by winds with a desired value of the magnetic field strength. It is important to estimate the filling factor of magnetised regions in this way, because it gives us the possibility to make simple predictions about where the magnetic fields may have

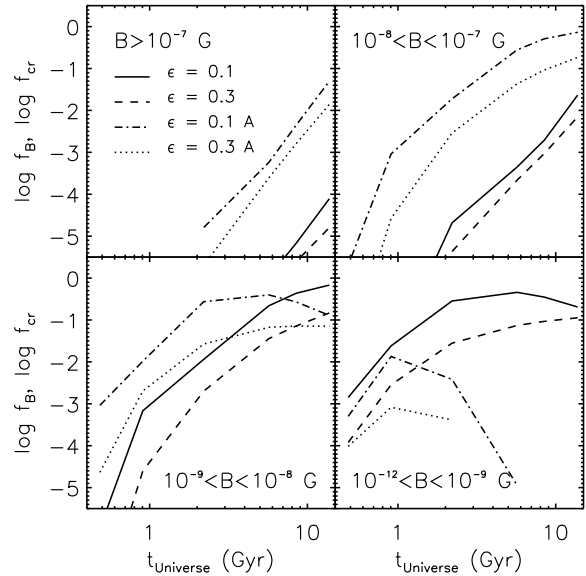


Figure 3. The volume filling factors of magnetised regions as a function of the cosmic time. The four panels show the filling factors of regions with magnetic field strengths in different ranges for all four models. Results also indicate the filling factors of the cosmic ray energy density in winds (see Subsection 4.1).

been ejected and transported by galactic winds and what kind of intensities we may expect them to have. Eventually, this gives us information about the ultimate mechanism that generated the magnetic fields we currently observe in the Universe. In the following, we will try to answer the questions: can galactic winds eject the seed magnetic fields that have generated the magnetic fields in clusters and in the IGM? Or do we need other mechanisms to explain them?

The volume filling factor f_B of magnetised regions is calculated using the same technique used by BSW05 to obtain the volume filling factor of galactic winds. Indeed, for each of our two models, the sum of the filling factors of regions with different magnetisation intensities shown in Fig. 3 is exactly the volume filling factor f_v of winds for the two models with $(K; \epsilon) = (0.5; 0.1)$ and $(K; \epsilon) = (0.5; 0.3)$ shown in Fig. 8 of BSW05. To calculate f_B we superpose a grid with 512³ pixels over our simulated region and we identify all those pixels which correspond to the desired magnetic field intensity. The volume filling factor is then simply given by the ratio between the number of pixels with the required magnetic field strength B and the total number of pixels in the grid. The magnetic field strength in each pixel is recovered by summing up the magnetic energy density of each wind intersecting that particular pixel and afterwards converting it into B using equation (11). This conversion assumes that the magnetic field energy is uniformly distributed inside winds: this is only statistically correct.

Our estimates for the volume filling factors of magnetised regions as a function of the cosmic time are shown in Fig. 3 for all models. The four panels represent the volume filling factors of regions with magnetic fields in four different intervals: i) $B > 10^{-7}$ G; ii) $10^{-8} < B < 10^{-7}$ G, iii) $10^{-9} < B < 10^{-8}$ G and iv) $10^{-12} < B < 10^{-9}$ G, respec-

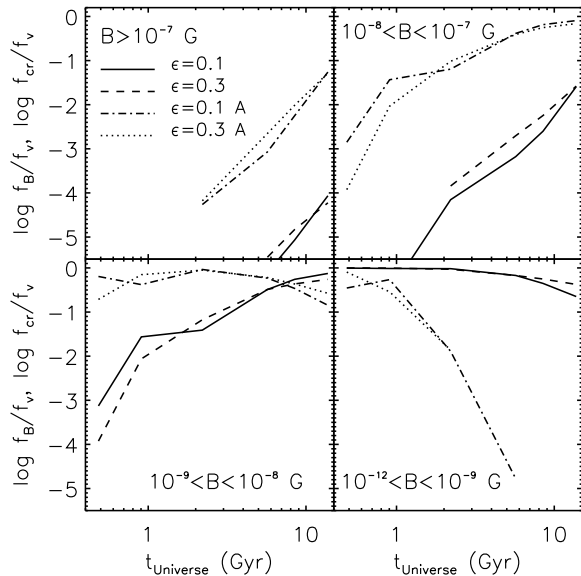


Figure 4. The relative volume filling factors of magnetised regions as a function of the cosmic time. The four panels show the filling factors of regions with magnetic field strengths in different ranges for all four models. Results also indicate the relative filling factors of the cosmic ray energy density in winds (see Subsection 4.1).

tively. Magnetic fields with strengths higher than 10^{-7} G have extremely low or low filling factors at all epochs in both scenarios. On the other hand, the total filling factor of magnetic fields with strengths in the range $10^{-12} < B < 10^{-7}$ G is already significant at $z \sim 3$ and approaches unity at the present epoch in models with $\varepsilon = 0.1$. This implies that in the $\varepsilon = 0.1$ and in the $\varepsilon = 0.1A$ models corresponding to efficient winds, the ejected magnetic fields permeate most of the universe at $z \sim 0$.

In Fig. 4 we show the relative volume filling factors of magnetic fields with given strengths as a function of cosmic time. We calculate the relative volume filling factor of magnetised regions with strengths in the same intervals used in Fig. 3. This quantity represents the ratio between the filling factors f_B shown in Fig. 3 and the total volume filling factor of galactic winds f_v as a function of time, that is $f = f_B/f_v$. f_v is the fraction of our simulated region affected by winds, independently of their magnetisation. Physically, f indicates the fraction of space affected by winds in which there is a magnetic field of a given intensity. It appears that in the conservative scenario only a tiny fraction (less than 10^{-4}) of the volume filled by winds contains magnetic fields higher than 10^{-7} G, while most of the wind filled regions have $10^{-12} < B < 10^{-8}$ G throughout the history of the Universe. In the conservative models, most magnetised regions have a magnetic fields smaller than about 10^{-9} G and only at the present time most regions can reach level of magnetisations as high as $B \sim 10^{-8}$ G.

On the other hand, in the optimistic models, most winds have magnetic field strengths in the range $10^{-9} < B < 10^{-7}$. In this models, at $z = 0$ most magnetised regions appear to have a magnetic field in the range $10^{-8} < B < 10^{-7}$ G

and almost no regions are only weakly magnetised (that is $B < 10^{-9}$ G). In particular, in the $\varepsilon = 0.1$ and in the $\varepsilon = 0.1A$ models, most of the Universe is highly magnetised at $z \sim 0$. If this were the case, galactic winds would be proven to be an efficient mechanism to explain the magnetisation of filaments and the IGM observed by Kim et al. (1989) and Bagchi et al. (2002), if cosmic shear or other amplification mechanisms could further amplify the seed fields by a factor of 10–1000.

Fig. 5 shows slices of the magnetic field evolution in our simulated region as a function of redshift. Results are presented for the $\varepsilon = 0.3$ (left panels) and $\varepsilon = 0.1$ (right panels) models of the conservative scenario. In the optimistic scenario models with $\varepsilon = 0.3A$ and $\varepsilon = 0.1A$, results are qualitatively similar, but the colour table would have to be stretched to higher values of the magnetic field intensity. From top to bottom and from left to right, the redshifts of the snapshots are $z = 3$, $z = 1$, $z = 0.5$ and $z = 0$. We cut a thin slice with a side of $52 h^{-1}$ Mpc through our simulated region and we colour-code the magnetic field strength from white (no field) to black (strongest fields). The value of the magnetic field in each pixel is the integrated value of the magnetic field B recovered in the 3D grid with 512^3 cells used to calculate the filling factors of magnetised regions in Subsection 3.2. There is a substantial difference between the maps of the magnetic fields in the two wind models shown here. Although the total volume filling factors f_v differ by less than an order of magnitude, the effect is clearly visible in Fig. 5. This again is a consequence of the efficiency of galaxies to blow winds, as determined by the parameter ε . In the $\varepsilon = 0.1$ model, winds fill almost all the simulated region, leaving us only a small chance, if any, to observe primordial magnetic fields in the Universe at $z \sim 0$. On the contrary, models with higher entrainment fraction parameters and less efficient winds as the $\varepsilon = 0.3$ model, show that although the winds do fill a large portion of the simulated volume, at least half or more of the intergalactic space is not affected by feedback from galactic outflows. This means that, in principle and with the appropriate experiment, one could observe primordial magnetic fields even in the present-day Universe.

The distribution of the magnetic fields in Fig. 5 shows clearly that they are not statistically homogeneously distributed in space, but that the magnetisation is somewhat correlated with the underlying large scale structure of matter and galaxies. This is easily understandable, because most of the galaxies blowing winds form in regions of relatively high density, like filaments and groups, while fewer objects populate very low density regions like voids. Therefore, it may be possible that the plasma in voids is still pristine, allowing to search for uncontaminated primordial magnetic fields. The probability to detect pristine gas in low density regions at $z = 0$ ranges from about 10% for the two models with $\varepsilon = 0.1$ to about 70% for the two models with $\varepsilon = 0.3$.

3.3 Further amplification of the Seed Magnetic Fields

In our simulations, most magnetised winds emerge from galaxies in filaments or galaxies that reside in proximity of regions with enhanced densities. Incidentally, these regions are also those where one would expect the amplifica-

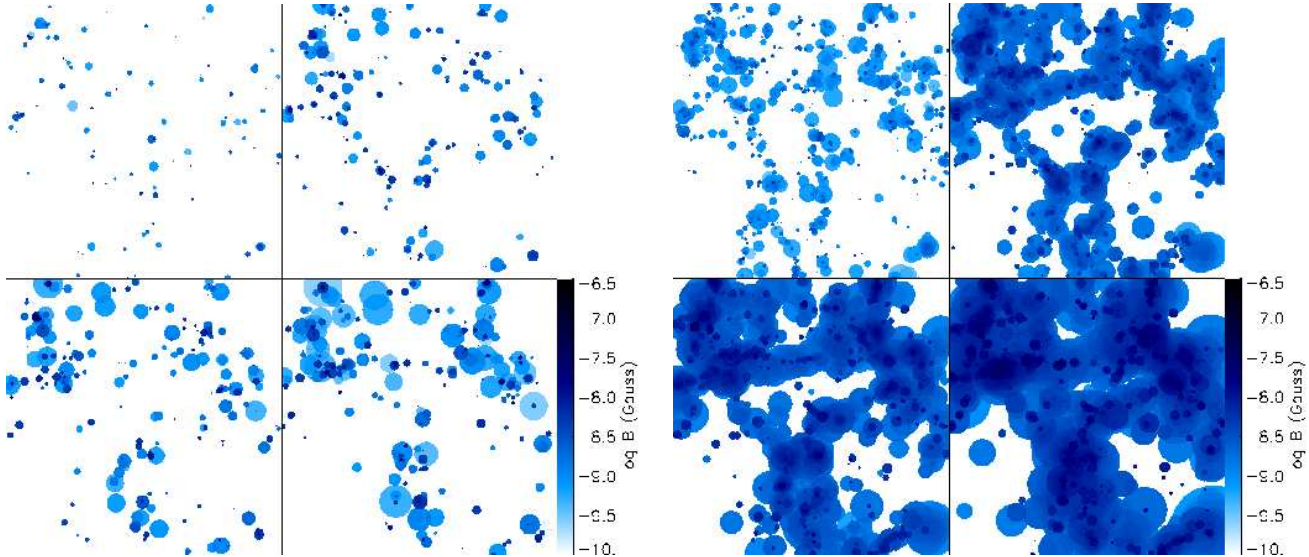


Figure 5. The evolution of the magnetic field strength with cosmic time. Results are presented for the wind models with $\varepsilon = 0.3$ (left panels) and with $\varepsilon = 0.1$ (right panels) of our conservative scenario. The initial injected magnetic field is $B_{\text{in}} = 1 \mu\text{G}$. In each figure, from top to bottom and left to right, the redshifts of the shown snapshots are $z = 3$, $z = 1$, $z = 0.5$ and $z = 0$ respectively. The colour coding is the same for all snapshots and for both models. The comoving dimension of the simulated region is $52 h^{-1} \text{ Mpc}$.

tion mechanisms such as cosmic shear and dynamo effects to be more efficient, because of the stirring of shear flows and turbulence by the infall of matter on the newly forming structures.

Clusters of galaxies are expected to be only weakly rotating, if at all, and other field amplification mechanisms than the $\alpha - \Omega$ dynamo have to be found to explain the observed magnetic fields. Jaffe (1980) and Ruzmaikin, Sokolov & Shukurov (1989) suggested that magnetic fields could be amplified by the small scale turbulence produced by the motion of galaxies through the ICM. However, De Young (1992) and Goldschmidt & Rephaeli (1993) demonstrate that this mechanism alone cannot fully produce the levels of magnetic fields observed in clusters.

There is some observational evidence for the existence of turbulence in clusters. Schuecker et al. (2004) find hints of the presence of turbulence in the Coma cluster by analysing the pressure fluctuations revealed by X-ray observations. Enßlin & Vogt (2005) suggest that hydrodynamical turbulence may be responsible for the generation of the Kolmogoroff-like magnetic power spectrum observed in the Hydra A cluster (Vogt & Enßlin 2005).

The merging of galaxy clusters is probably the most important source of turbulence in the ICM (Tribble 1993, Roettiger, Burns & Stone 1999, Norman & Bryan 1999). Roettiger, Stone & Burns (1999) find that magnetic fields can be amplified three times more efficiently in clusters with ongoing mergers. Dolag, Bartelmann & Lesch (1999) and Dolag, Bartelmann & Lesch (2002) simulate the magnetic field evolution in clusters and find that the field strength can be increased by factors of order 10^3 by compression and shear of random flows during the cluster formation. Such an amplification factor would be sufficient to bring even the seed magnetisation of a nG we find in our conservative models to the observed μG level of magnetisation in galaxy clusters.

Galactic winds emerging from galaxies in clusters can

contribute to the magnetisation of the ICM in clusters even when they do not escape the gravitational attraction of the halo. In fact, when star formation occurs, some material can be shocked and ejected outside the plane of the galaxy. This gas is then quickly stripped away from the galaxy by the ram pressure of the hot cluster gas (Soker, Bregman & Sarazin 1991, Gaetz, Salpeter & Shaviv 1987) and mixed into the ICM. The stripped material would therefore contribute to chemically enrich, shock heat and magnetise the ICM of the cluster, although it would be unable to power a wind and reach the IGM. Unfortunately, we are currently unable to reproduce this effect in our numerical model.

Outside clusters and bound structures, magnetic fields in winds can be amplified by turbulence, if present, by the cosmic shear and by the compression of the outflowing gas into a thin shell, when winds become momentum-driven and evolve like a snowplough. In this last case, the density of the cooled material accumulating onto the shells, which is a mixture of supernova ejecta, shocked interstellar medium and gas accreted from the ambient medium, can become much higher than the density of the ambient medium. Shell overdensities δ are usually in the range $4\bar{\rho}_{\text{baryons}} < \delta < 1000\bar{\rho}_{\text{baryons}}$. This compression of the gas in shells produces and analogous compression of the magnetic field lines associated with the outflowing gas, which in turn can locally amplify the magnetic fields. We do not attempt to model this effect in our simulations.

4 EXTRAGALACTIC COSMIC RAYS

Cosmic rays, the other non-thermal component of the intergalactic and intracluster gas, are relativistic charged particles and, as such, they are strongly coupled to magnetic fields. Cosmic ray electrons are currently observed through the synchrotron radiation that they emit when spiralling around the magnetic field lines. Since their cooling time

is dominated by the energy losses from Compton scattering and/or synchrotron emission, energetic cosmic ray electrons cool fast, limiting the observability of the primary cosmic ray electrons to a short period of their lifetime. Cosmic ray protons have not yet been unambiguously detected, but new and up-coming gamma-ray telescopes, such as the High Energy Gamma Ray Astronomy (HEGRA), the Gamma Ray Large Area Space Telescope (GLAST), the High Energy Stereoscopic System (H.E.S.S.) telescope, and the Major Atmospheric Gamma Imaging Cherenkov Telescope (MAGIC), are aimed to detect them from the gamma rays produced in hadronic interactions with the intergalactic and intracluster gas. The relativistic electrons and positrons generated by hadronic proton-proton collisions are one, among others, viable explanation of the cluster-sized diffuse radio haloes, observed in a significant fraction of galaxy clusters (Dennison 1980; Vestrand 1982; Blasi & Colafrancesco 1999; Dolag & Enßlin 2000; Pfrommer & Enßlin 2004a). The amount of cosmic ray energy required to power those radio haloes is moderate and comparable to the expected magnetic field energy (Pfrommer & Enßlin 2004b). Since cosmic ray protons are confined by chaotic magnetic field lines, they are likely to accumulate in turbulent regions of the Universe, and especially in clusters (Völk, Aharonian & Breitschwerdt 1996; Enßlin et al. 1997; Berezhinsky, Blasi & Ptuskin 1997; Völk & Atoyan 2000).

4.1 Predictions for Cosmic Rays

In our own Galaxy, the cosmic ray energy density is of order of the magnetic energy density (Beck 2001). In general, the cosmic rays that accumulate over cosmic times should be relativistic, since sub-relativistic protons can suffer from severe Coulomb energy losses in the dense ISM and ICM (e.g. Enßlin et al. 1997). If we take this into account, we can approximate the equation of state of the cosmic ray gas with a polytrope with adiabatic index $\gamma_{\text{CR}} = 4/3$. This implies that the cosmic ray-producing gas suffers exactly the same (relative) adiabatic energy losses as the (turbulent) magnetic fields. Thus, we can assume that the cosmic ray energy injected in winds is identical to the magnetic energy density and in our wind description we can read any magnetic field energy density also as a cosmic ray energy density, that is $\varepsilon_{\text{CR}} = \varepsilon_{B_{\text{in}}} = B^2 / (8\pi)$.

Our prescriptions for winds assume that the outflows are (initially) thermally driven, and not cosmic ray-driven (Dorfi 2004, Breitschwerdt, Voelk & McKenzie 1991). We also implicitly assume that the thermal and the relativistic components of the plasma outflowing from galaxies are not coupled via Alfvén waves. If this were to happen, the cosmic rays would contribute momentum to the wind and an appropriate term \dot{E}_{CR} should be included in equation 2. This injection of momentum by cosmic rays could in principle provide a wind with the necessary kick to escape from a galaxy where star formation is not very intense.

The equipartition of energy between magnetic fields and cosmic rays may not be true in all environments. In cosmic ray-driven outflows, for example, the cosmic rays leave the galaxy without ejecting much gas or magnetic fields. In this case, the contribution of winds to the cosmic ray content of the ICM and IGM could be much higher than our estimate.

Hence, our results about the ejection of cosmic rays should be treated as lower limits.

The small energy density in injected cosmic rays can also be substantially boosted by the action of structure formation. It is expected that every gas volume in the IGM which ends up in the ICM is passed by shock waves of different strength several times. Many of these shock waves have low Mach numbers, implying that they are very inefficient in accelerating particles out of the thermal pool. However, any pre-existing relativistic particle population is able to gain substantial energy by the passage of even weak shocks (e.g. Miniati et al. 2001a,b). Furthermore, resonant interactions with turbulent plasma waves can also energise old cosmic ray populations to some degree (Brunetti et al. 2001, 2004). We do not attempt an estimate of the cosmic ray amplification processes. However, it is possible that also these seed cosmic rays may have become an energetic population at present days.

5 CONCLUSIONS

We have presented new semi-analytic simulations of magnetised galactic winds emerging from star forming galaxies. Our set of N-body simulations of structure formation in an approximately spherical region of space of diameter $52 h^{-1}$ Mpc combines a high mass resolution with a region of space large enough to allow us to simulate the evolution of the winds in their proper cosmological context. We have implemented new recipes for the transport of magnetic fields into the IGM and ICM by outflows on top of the pre-existing semi-analytic scheme for the evolution of winds of BSW05, which uses the galaxy formation model of Springel et al. (2001).

The assumption that the magnetic fields only weakly affect the global evolution of winds is well justified by the finding that the total energy of the outflow is several orders of magnitude higher than its magnetic energy. Here we have presented two different scenarios for the transport of magnetic fields in winds and for each scenario we have analysed two models corresponding to high and low wind efficiency to blow and travel far into the IGM. As shown in Bertone, Stoehr & White (2005), the ability of winds to travel far into the IGM strongly depends on their mass loading efficiency: the more mass is accreted from the ambient medium, the lower is the probability that winds can blow out of galaxies. The mass loading efficiency is parameterized in the wind model by the constant ε . Unfortunately, no direct observational evidence is available to constrain this parameter.

In both scenarios, we have neglected any possible field amplification process due to cosmic shear and turbulence in clusters. These processes are far too complex to be treated correctly in semi-analytic models. In what we called our conservative scenario we do not consider any amplification mechanism, but we take into account the dilution of the magnetic fields due to the adiabatic expansion of the magnetic field lines inside winds. This implies that the results of our conservative models should be regarded as lower limits to any seed magnetisation of the Universe. Conversely, in our optimistic scenario we do consider a simple prescription for the amplification of magnetic fields in winds, due to

the shear motions of the material inside the wind cavities and bubbles. In the two optimistic models, we consider an efficient amplification of the magnetic fields by the internal shear motions and we set up our prescriptions by assuming that the amplification by shear motions counterbalances the dilution due to the adiabatic expansion.

Since cosmic rays can be strongly coupled to turbulent magnetic fields, the simulations also allow us to follow the seeding of cosmic rays by galactic winds in the IGM and ICM. Given our assumption that the magnetic energy density equals the cosmic ray energy density, in our simulations the cosmic rays are spatially distributed in the same way as the magnetic fields.

We find that the magnetic fields ejected by galaxies with stellar masses $M_\star \gtrsim 10^8 M_\odot$ can fill a substantial fraction of our simulated volume, producing a mean (seed) magnetisation of order 10^{-12} to 10^{-8} G in the conservative models and of order 10^{-9} to 10^{-7} G in the optimistic models. Magnetic field are not uniformly distributed in space, but rather seem to roughly follow the large scale distribution of the underlying dark matter density field.

The ejection of magnetic fields and cosmic rays by galactic winds is efficient enough to explain the magnetic fields and cosmic ray energy densities observed or expected in clusters, if additional mechanisms intervene to amplify the magnetic fields and to energise the cosmic rays by a further factor of 10 to 1000. Amplification mechanisms such as cosmic shear, dynamo effects and others (see Section 3.3 for a discussion) do operate while the fields are ejected by winds into the ICM and IGM. It remains to be shown, however, whether the cosmic ray protons transported by winds can be re-accelerated by intergalactic shocks and turbulence to the level expected in galaxy clusters from the existence of radio haloes, which might be of hadronic origin.

Our model does not exclude *a priori* an additional primordial magnetic field. In fact, since at least in the high mass loading wind scenario a non-negligible fraction of our simulated volume is unaffected by magnetised winds, it may in principle be possible to detect primordial magnetic fields in those regions which have not been affected by feedback effects.

ACKNOWLEDGEMENTS

We would like to thank Felix Stoehr for his M3 simulations and Andrew Liddle and Simon White for reading the manuscript. This work has been supported by the Research and Training Network “The Physics of the Intergalactic Medium” set up by the European Community under contract HPRN-CT-2000-00126. SB was partially supported by PPARC.

APPENDIX A: DERIVATION OF THE MAGNETIC ENERGY EVOLUTION EQUATION

In this section we derive the equation for the evolution of the magnetic energy in winds. We introduce the set of approximations necessary to yield the evolutionary equations used in our simulations (Equations 7 and 15). This derivation

should both motivate our approach and clearly show where its limitations are.

We first consider the magnetic induction equation:

$$\frac{\partial \vec{B}}{\partial t} = \vec{\nabla} \times \vec{v} \times \vec{B} \quad (\text{A1})$$

From this, we easily obtain the evolution equation of the magnetic energy density $\varepsilon_B = B^2/(8\pi)$

$$\frac{d\varepsilon_B}{dt} = \frac{-B^2 \vec{\nabla} \cdot \vec{v} + \vec{B} \cdot \vec{B} : \vec{\nabla} \vec{v}}{4\pi}, \quad (\text{A2})$$

where $d/dt = \partial/\partial t + \vec{v} \cdot \vec{\nabla}$ is the total time (or convective) derivative. The magnetic energy stored in the wind is

$$E_B \equiv E_B[V_w] = \int_{V_w} d^3x \varepsilon_B = V_w \langle \varepsilon_B \rangle_{V_w}, \quad (\text{A3})$$

where $\langle \dots \rangle_{V_w}$ denotes the average over the wind volume V_w . The magnetic field strength of winds provided in the paper should be understood in terms of this average.

We are interested in the time derivative of $E_B[V_w]$, for which we need the variation of the energy density and of the volume. Since the latter is the integration volume and therefore non-trivially differentiable, one best introduces a coordinate system $\vec{x}(t)$, co-moving with the gas flow, which is the solution of the equation $\dot{\vec{x}}(t) = \vec{v}(\vec{x}, t)$, with the initial condition $\vec{x}(t_0) = \vec{x}_0$. This allows a coordinate transformation to the static coordinate system \vec{x}_0 , so that the energy density in a sub-volume V of V_w evolves accordingly to:

$$\begin{aligned} \frac{d}{dt} E_B[V] &= \frac{d}{dt} \int_{V_0} d^3x_0 \left| \frac{\partial \vec{x}}{\partial \vec{x}_0} \right| \varepsilon_B(\vec{x}(\vec{x}_0, t), t) \\ &= \int_V d^3x \frac{d}{dt} \varepsilon_B(\vec{x}, t) + \int_V d^3x \varepsilon_B(\vec{x}, t) \left| \frac{\partial \vec{x}_0}{\partial \vec{x}} \right| \\ &\quad \left(\left| \frac{\partial(v_x, y, z)}{\partial \vec{x}_0} \right| + \left| \frac{\partial(x, v_y, z)}{\partial \vec{x}_0} \right| + \left| \frac{\partial(x, y, v_z)}{\partial \vec{x}_0} \right| \right) \\ &= \int_V d^3x \frac{d}{dt} \varepsilon_B + \int_V d^3x \varepsilon_B \vec{\nabla} \cdot \vec{v} \\ &= \int_V \frac{d^3x}{8\pi} (2 \vec{B} \cdot \vec{B} : \vec{\nabla} \vec{v} - B^2 \vec{\nabla} \cdot \vec{v}). \end{aligned} \quad (\text{A4})$$

The second equation is obtained by transforming back to the original coordinate \vec{x} , while the third equation can be derived by using the product rule of determinants and explicit calculation. Let us imagine that the wind volume can be split into a number N of sub-volumes V_i : within each sub-volume the magnetic field can be assumed to be statistically homogeneous. We can therefore write

$$E_B[V_w] = \sum_i^N E_B[V_i] = \sum_i^N V_i \varepsilon_{B_i} \quad (\text{A5})$$

and introduce the rescaled field strength $\vec{b} = \vec{B}/B_i$. The time derivative is then

$$\frac{d}{dt} E_B = \sum_i^N \frac{d}{dt} E_B[V_i] + \frac{dN}{dt} E_B[V_{N+1}], \quad (\text{A6})$$

where the last term accounts for the injection of a new wind volume element V_{N+1} at the base of the wind. We identify this term with $\dot{E}_{B_{\text{in}}} = \varepsilon_{B_{\text{in}}} \dot{V}_{\text{in}}$.

Finally, to derive the simplified Equation 7 for the magnetic energy evolution, some further idealised approximations are necessary:

(i) **Vanishing cross correlation** between fluid motion and magnetic fields.

(ii) **Statistical isotropy** of the magnetic fields, which implies $\langle \vec{b} \vec{b} \rangle_{V_i} = \frac{1}{3} \mathbf{1}$.

In order to make the impact of these idealisations more transparent, we transform Eq. A6 so that it can be split into an ideal and a non-ideal part,

$$\frac{d}{dt} E_B = \dot{E}_{B_{\text{in}}} - \frac{E_B}{3} \frac{\dot{V}_w}{V_w} + \sum_i^N E_{B_i} \left[\frac{1}{3} \left(\frac{\dot{V}_w}{V_w} - \frac{\dot{V}_i}{V_i} \right) \langle (b^2 - 1) \vec{\nabla} \cdot \vec{v} \rangle_{V_i} + \frac{2}{3} \langle \vec{b} \vec{b} \rangle_{V_i} \frac{\mathbf{1}}{3} \right] \text{ (A7)}$$

where the ideal part (including the left-hand side term and the first two right-hand side terms) is identical to Eq. 7. The non-ideal part includes three contributions. The first term accounts for deviations of the relative expansion of different regions from the overall expansion rate. This term is probably small during the pressure-driven phase of the wind expansion, but will lead to a larger inaccuracy of our simplified description during the momentum-driven phase, when the different regions of the wind expand in a different way. The second term accounts for correlations in the expansion rate within the sub-volumes with the magnetic field strength. For dynamically unimportant fields, we expect this term to be small. For dynamically important field strengths, we expect the magnetic structures to expand faster than the unmagnetized regions, leading to an overestimate of the field strength. However, the basic assumption of our description is that within the wind volume (which excludes the base of the wind) magnetic fields are not dynamically important. These two non-ideal contributions vanish if no correlation exists between the magnetic fields and the fluid motion both on large and small scales. The third non-ideal contribution is due to the shearing of the magnetic fields and leads in general to a field amplification. This term vanishes if the fields are both isotropic and uncorrelated with the fluid motion. Otherwise, it should lead to dynamo action, for which we account in Eq. 15 with a very simplified but effective description.

REFERENCES

Adelberger K.L., Steidel C.C., Shapley A.E., Pettini M., 2003, ApJ, 584, 45

Aguirre A., Hernquist L., Schaye J., Katz N., Weinberg D.H., Gardner J., 2001, ApJ, 561, 521

Aguirre A., Schaye J., Hernquist L., Kay S., Springel V., Theuns T., 2005, ApJ, 620, 13

Bagchi J., Enßlin T. A., Miniati F., Stalin C. S., Singh M., Raychaudhury S., Humeshkar N. B., 2002, New Astronomy, 7, 249

Beck R., 2001, Space Science Reviews, 99, 243

Berezinsky V. S., Blasi P., Ptuskin V. S., 1997, ApJ, 487, 529

Bertone S., Stoehr F., White S.D.M., 2005, MNRAS, 359, 1201 (BSW05)

Bertone S., White S.D.M., 2005, MNRAS, in press

Birk G. T., Wiechen H., Otto A., 1999, ApJ, 518, 177

Blasi P., Colafrancesco S., 1999, Astroparticle Physics, 12, 169

Breitschwerdt D., Voelk H.J., McKenzie J.F., 1991, A&A, 245, 79

Brunetti G., Setti G., Feretti L., Giovannini G., 2001, MNRAS, 320, 365

Brunetti G., Blasi P., Cassano R., Gabici S., 2004, MNRAS, 350, 1174

Carilli C. L., Taylor G. B., 2002, ARA&A, 40, 319

Cecil G., Bland-Hawthorn J., Veilleux S., 2002, ApJ, 576, 745

Chakrabarti S. K., Rosner R., Vainshtein S. I., 1994, Nature, 368, 1434

Chyžík K., Beck R., 2004, A&A, 417, 541

Chyžík K. T., Knapik J., Bomans D.J., Klein U., Beck R., Soida M., Urbanik M., 2003, A&A, 405, 513

Ciardi B., Stoehr F., White S.D.M., 2003, MNRAS, 343, 1101

Clarke T. E., Kronberg P. P., Böhringer H., 2001, ApJL, 547, 111

Dahlem M., Petr M.G., Lehnert M.D., Heckman T.M., Ehle M., 1997, A&A, 320, 731

Daly R. A., Loeb A., 1990, ApJ, 364, 451

De Young D. S., 1992, ApJ, 386, 464

Dennison B., 1980, ApJL, 239, 93

Dreher J. W., Carilli C. L., Perley R. A., 1987, ApJ, 316, 611

Dolag K., Bartelmann M., Lesch H., 1999, A&A, 348, 351

Dolag K., Enßlin T. A., 2000, A&A, 362, 151

Dolag K., Bartelmann M., Lesch H., 2002, A&A, 387, 383

Dolag K., Vogt C., Enßlin T. A., 2005, MNRAS, 358, 726

Dorf E. A., 2004, Ap&SS, 289, 337

Enßlin T. A., Biermann P. L., Kronberg P. P., Wu X., 1997, ApJ, 477, 560

Enßlin T. A., Vogt C., 2003, A&A, 401, 835

Enßlin T. A., Vogt C., 2005, arXiv:astro-ph/0505517

Frye B., Broadhurst T., Benitez N., 2002, ApJ, 568, 558

Gaetz T. J., Salpeter E. E., Shaviv G., 1987, ApJ, 316, 530

Goldshmidt O., Rephaeli Y., 1993, ApJ, 411, 518

Golla G., Hummel., 1994, A&A, 284, 777

Govoni F., Feretti L., 2004, Int. Journ. of Mod. Phys. D, 13, 1549

Hoyle F., 1969, QJRAS, 10, 10

Jaffe W., 1980, ApJ, 241, 925

Kapferer W., Ferrari C., Domainko W., Mair M., Kronberger T., Schindler S., Kimeswenger S., van Kampen E., Breitschwerdt D., Ruffert M., 2006, A&A, 447, 827

Kauffmann G., Colberg J.M., Diaferio A., White S.D.M., 1999, MNRAS, 303, 188

Kim K.-T., Kronberg P. P., Giovannini G., Venturi T., 1989, Nature, 341, 720

Kim K.-T., Kronberg P. P., Dewdney P. E., Landecker T. L., 1990, ApJ, 355, 29

Kronberg P. P., 1994, Rep. Prog. Phys., 57, 325

Kronberg P. P., Lesch H., Hopp U., 1999, ApJ, 511, 56

Kronberg P. P., Dufton Q. W., Li H., Colgate S. A., 2001, ApJ, 560, 178

Harnett J., Ehle M., Fletcher A., Beck R., Haynes R., Ryder S., Thierbach M., Wielebinski R., 2004, A&A, 421, 571

Heckman T.M., Lehnert M.D., Strickland D.K., Armus L., 2000, ApJS, 129, 493

Johnston-Hollitt M., Ekers R. D., 2004 pre-print astro-ph/0411045

Madau P., Ferguson H.C., Dickinson M.E., Giavalisco M., Steidel C.C., Fruchter A., 1996, MNRAS, 283, 1388

Martin C.L. 1999, *ApJ*, 513, 156

Miniati F., Jones T. W., Kang H., Ryu D., 2001a, *ApJ*, 562, 233

Miniati F., Ryu D., Kang H., Jones T. W., 2001b, *ApJ*, 559, 59

Norman M. L., Bryan, G. L., 1999, *Lecture Notes in Physics* Vol. 530: The Radio Galaxy Messier 87, 530, 106

Ostriker J. P., McKee C. F., 1988, *Rev. Mod. Phys.*, 60, 1

Pfrommer C., Enßlin T. A., 2004a, *A&A*, 413, 17

Pfrommer C., Enßlin T. A., 2004b, *MNRAS*, 352, 76

Phillips A.C., 1993, *AJ*, 105, 486

Rees M., 1987, *QJRAS*, 28, 197

Reuter H.-P., Klein U., Lesch H., Wielebinski R., Kronberg P. P., 1992, *AAP*, 256, 10

Roettiger K., Stone J. M., Burns J. O., 1999, *ApJ*, 518, 594

Roettiger K., Burns J. O., Stone J. M., 1999, *ApJ*, 518, 603

Reuter H.-P., Klein U., Lesch H., Wielebinski R., Kronberg P. P., 1994, *A&A*, 282, 742

Schuecker P., Finoguenov A., Miniati F., Böhringer H., Briel U. G., 2004, *A&A*, 426, 387

Ruzmaikin A., Sokolov D., Shukurov A., 1989, 241, 1

Shu C., Mo H. J., Mao S., 2005, *ChJAA*, 5, 327

Soida M., Urbanik M., Beck R., Wielebinski R., Balkowski C., 2001, *A&A*, 378, 40

Soker N., Bregman, J. N., Sarazin C. L., 1991, *ApJ*, 368, 341

Springel V., White S. D. M., Tormen G., Kauffmann G., 2001, *MNRAS*, 328, 726

Springel V., Yoshida N., White S. D. M., 2001, *New Astronomy*, 6, 79

Subramanian K., 1999, *PhRvL*, 83, 2957

Stoehr F., 2003, PhD Thesis, Ludwig Maximilian Universität, München

Taylor G. B., Perley R. A., 1993, *ApJ*, 416, 554

Theuns T., Viel M., Kay S., Schaye J., Carswell R.F., Tzanavaris P., 2002, *ApJL*, 578, 5

Tribble P. C., 1993, *MNRAS*, 263, 31

Tüllmann R., Dettmar R.-J., Soida M., Urbanik M., Rossa J., 2000, *A&A*, 364, 36

Veilleux S., Cecil G., Bland-Hawthorn J., 2005, *ARA&A*, 43, 769

Vestrand W. T., 1982, *AJ*, 87, 1266

Vogt C., Enßlin T. A., 2005, *A&A*, 434, 67

Vogt C., Enßlin T. A., 2003, *A&A*, 412, 373

Vogt C., Dolag K., Enßlin T. A., 2005, *MNRAS*, 358, 732

Völk H. J., Aharonian F. A., Breitschwerdt D., 1996, *Space Science Reviews*, 75, 279

Völk H. J., Atoyan A. M. 2000, *ApJ*, 541, 88

Widrow L. M., 2002, *Reviews of Modern Physics*, 74, 775